Available online at www.sciencedirect.com
SCIENCE DIRECT®
PERGAMON
International Journal of Heat and Mass Transfer 46 (2003) 1519–1528
International Journal of HEAT and MASS TRANSFER
www.elsevier.com/locate/ijhmt

Nonlinear analysis on fluctuation feature of two-phase flow through a T-junction

S.F. Wang [a,*], R. Mosdorf [b,1], M. Shoji [a,2]

[a] Department of Mechanical Engineering, Graduate School of Engineering, The University of Tokyo, 7-3-1 Hongo, Bunkyo-ku, Tokyo 113-8656, Japan

[b] Faculty of Computer Science, Bialystok University of Technology, 15-351 Bialystok, ul. Wiejska, Poland

Received 22 April 2002; received in revised form 25 October 2002

Abstract

Several measurement methods of chaos dynamics were employed to analyze differential pressure fluctuations of two-phase flow through a T-junction with the aim to make clear the two-phase flow behavior splitting at a T-junction. These results may be significant for better understanding the flow structure and also for establishing valid models different from conventional viewpoints. These methods included: power spectral density and Hurst exponent, Lyapunov exponent, correlation dimension, pseudo-phase-plane trajectory. The experimental test section is a symmetrical and vertical impacting T-junction with 15 mm inner diameter for the main tube and two horizontal branches. Three kinds of flow pattern including bubble flow, churn flow and annular flow in the inlet tube, were investigated by detecting time series of differential pressure. It is demonstrated that two-phase flow splitting at a T-junction is a complicated nonlinear dynamic system. The Hurst exponents were larger than 0.5 showing that the flow behaviors studied are partly chaotic. The largest Lyapunov exponent greater than zero confirms the chaotic feature of two-phase flow at a T-junction in quality. Correlation dimensions were used to quantify the identified chaotic behavior.

Keywords: Two-phase flow; T-junction; Nonlinear dynamic; Chaotic behavior

1. Introduction

T-junctions are commonly used in distributing two-phase flow by piping networks. These networks are essential components of many facilities in the power and process industries, such as steam power plants, boiling-water and pressured water nuclear reactors and a wide variety of chemical and petroleum applications. Understanding the behavior of two-phase flow through a T-junction is extremely important since it can have significant effects on the operation, maintenance and efficiency of all components downstream from the junction.

In the past years, scientific research on behaviors of two-phase flow through a T-junction has been mainly concentrated on phase distribution and the pressure drop. Four state-of-the-art reviews [1–5] summarized the research efforts in the recent literature excellently. These research efforts have shown that the phases are not distributed evenly at the junction and the pressure drops associated with two-phase flow are significantly complicated with much higher magnitudes comparing to single-phase. If we address only the research on the pressure drop, a lot of researchers in the past have devoted their efforts to experiments and modeling. Saba and Lahey [6] conducted experiments with air–water through a horizontal T-junction and developed physically-based empirical model to predict pressure drop for both ΔP_{13} (pressure drop from inlet 1 to outlet 3 of the

* Corresponding author. Tel./fax: +81-3-5841-6408.
E-mail addresses: wang@photon.t.u-tokyo.ac.jp (S.F. Wang), mosdorf@ii.pb.bialystok.pl (R. Mosdorf), shoji@photon.t.u-tokyo.ac.jp (M. Shoji).
[1] Tel.: +48-85-7428-206; fax: +48-85-7428-393.
[2] Tel.: +81-3-5841-6406; fax: +81-3-5800-6987.

0017-9310/03/$ - see front matter
PII: S0017-9310(02)00455-6

Nomenclature

A	cross-sectional flow area (m^2)
C	correlation integral
D	inlet diameter (m); correlation dimension
H	Hurst exponent
J_G	superficial gas velocity (m)
J_L	superficial liquid velocity (m)
l	distance in the phase space
M	embedding dimension
N	number of samples
ΔP_{12}	pressure drop from inlet 1 to outlet 2 of the junction (mm H_2O)
ΔP_{13}	pressure drop from inlet 1 to outlet 3 of the junction (mm H_2O)
R	difference between the maximum and minimum value of T
S	standard deviation
T	time series of cumulated value
W	mass flow rate (kg/s)
W_G	gas mass flow rate (kg/s)
W_L	liquid mass flow rate (kg/s)
X	quality ($= W_G/W_L$)
x	measured value
$\bar{x}$	mean value

Greek symbols

λ	Lyapunov exponent
τ	time lag (s)
Θ	Heaviside function
ρ	density (kg/m^3)

Subscripts

1, 2, 3	inlet 1, outlet 2, and outlet 3 of the T-junction, respectively (Fig. 2)
l	largest

junction) and ΔP_{12} (pressure drop from inlet 1 to outlet 2 of the junction). The model, however, is only valid for small conduits and for mass flow extraction ratio greater than 0.3, where W_1 and W_3 are the inlet and branch mass flow rates. Reimann and Seeger [7] measured the pressure drop ΔP_{13} and ΔP_{12} for air–water and steam water through several kinds of T-junction. They also established available models, and the agreement between the model and the experiments is good for the horizontal downward branch but bad for upward branch flow. Hwang and Lahey [8] conducted experiments with air–water for three horizontal junctions (T-junction, 45° Y-junction, and 135° Y-junction). A phenomenological model was developed basing on the idea of dividing streamlines, and good consistence was obtained between the model and experiment data. Ballyk et al. [9] reformed experiments with steam-water annular inlet flow in a horizontal T-junction. The pressure change ΔP_{12} was modeled using an axial momentum balance at the junction. ΔP_{13} was modeled using a balance of mechanical energy for the branching flow, which consisted of reversible and irreversible components. Ruell et al. [10] presented experimental data for pressure drops of air–water mixture at a horizontal T-junction. They made comparisons between their data and existing models. Excellent summary was proposed from these comparisons. Walters et al. [11] reported their experimental results on pressure drop of air–water in two reduced T-junctions. They concluded that, for ΔP_{12}, the separated flow model by Foude and Rhodes [12] gave the best overall predictions for all inlet flow patterns, except slug flow. For ΔP_{13}, the separated flow model proposed by [6] gave the overall predictions for both ΔP_{12} and ΔP_{13} test sections.

From the literature, we may say that few of the investigations deal with dynamic behaviors. Although the idealized case of the true stead-state will probably have to be well understood before the more complicated case can be considered, the neglect of the time-dependent behaviors of these parameters is acknowledged to be a departure from the physical reality [13,14]. So the objective of the present research is to understand the dynamic behaviors of two-phase flow through a T-junction by analyzing the time-dependent differential pressure signal with nonlinear dynamic methods. Although the intensity of fluctuation of two-phase flow through a T-junction has been analyzed by statistical methods in [15], it is still necessary to know the system complexity and configuration by nonlinear analysis. Furthermore, an attempt to apply chaos theory for the system of two-phase flow splitting at T-junctions has been made. Several measurement methods that are used in chaos theory such as Hurst dimensions, Lyapunov exponents, pseudo-phase-plane trajectory, power spectral density (PSD) function and correlation dimensions were employed on various inlet flow patterns. Since slug flow was not observed under the present experimental conditions, only bubble flow, churn flow and annular flow were discussed in the present paper.

2. Experimental apparatus and measurements

A schematic diagram of the two-phase flow through T-junction loop is shown in Fig. 1. The air, before entering the mixing room, was passed through a filter, pressure controller, and a set of rotameters (OMEGA with a combined range of 0.05–500 l/min) for large and

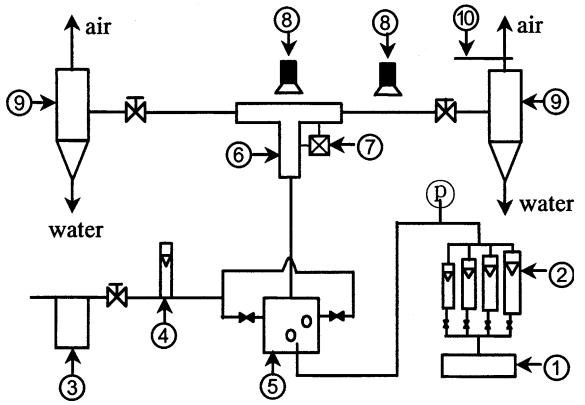

Fig. 1. Schematic diagram of experimental apparatus: (1) compressor (2) air flowmeters (3) filter (4) water flowmeter (5) mixingroom (6) T-junction (7) differential pressure sensor (8) high speed video (9) separator (10) hot wire anemometer.

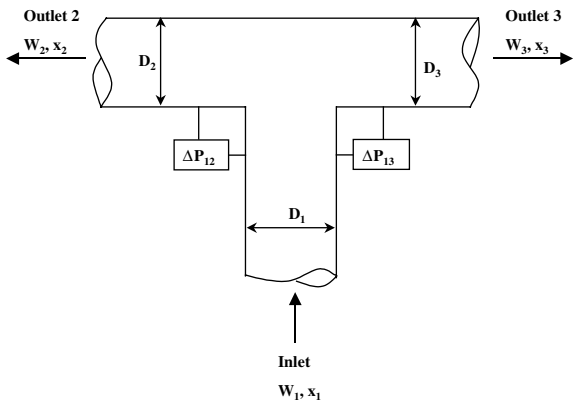

Fig. 2. Test section.

small range, whilst the water was supplied from the faucet passed through a filter and a rotameter (OMEGA with a range of 0–2 l/min). The mixing room consisted of an annular section surrounding a porous wall section. Water enters the room from the periphery whilst the air passes up from the middle. The vertical inlet tube upstream of the tee was 1.5 m high, which provided a length/hydraulic diameter ratio of 100. This length was sufficient to ensure that relatively developed air–water two-phase flow entered the T-junction. Two of the horizontal side branches were 1.7 m long. The vertical T-junction and the connecting tubes, inner diameters of which were 15 mm, were constructed of acrylic resin to permit visual and photographic observation. The outside of the T-shaped block has a square cross section to minimize the refraction problems during the observation of the flow. All rotameters for air and water were calibrated and compared with the manufacturer's calibration. Typical deviations between the two calibrations were found to be within ±2% with a maximum of ±5% at the lowest flow rates.

Pressure drop ΔP_{13} (between inlet 1 and to outlet 3) and ΔP_{12} (between inlet 1 and outlet 2) were obtained by Validyne DP15, differential transducer with maximum range of $\approx\pm225$ kg/cm^2 and a Validyne CD-280 pressure demodulator. Output from the pressure transducers was fed into the data-acquisition system in the form of a DC voltages signal (range ±12.29 V). An appropriate calibration equation was then used to convert the voltages into differential pressure. Because of the extreme sensitivity of these measurements, the calibration of the transducer was repeated several times during testing. Fig. 2 shows the test section. Pressure taps were employed to connect differential transducer with test tube. At each tap location, a 1mm hole was drilled through the tube wall, and short pieces of tubing were then bent for connecting the taps to the pressure measurement system. Special care was taken in drilling and polishing the taps to ensure no burrs protruded into the flow area. The tubes between tap and transducer were purged before each test to ensure that the lines were free of air. Gas flow rate at the branch outlet was measured by a hot-wire anemometer sampled simultaneously with differential pressure waveform. Both of the gas flow rate signal and differential pressure signal were obtained from samples taken over 60 s at a rate of 200 samples/s. Two high-speed video cameras were employed for visual observation. One was set at 1000 frames/s to record the behavior of the splitting flow at center area of the T-junction. The other was set at 500 frames/s to get the behavior of two-phase flow in branch tube. Both of the videos were recorded simultaneously with differential pressure signal and gas flow rate signal. About 30 min should be waited before each test run to reach the steady state. Water flow rate at the branch outlet was measured by weighting timed efflux. A steady interface in the separator was maintained while measurement was executed.

Mass balance errors were calculated for both phases as the percentage deviation between the inlet flow rate and the sum of the outlet flow rates from two separators. For air, the mass balance was maintained within ±10% in all test runs, and within ±5% for 80% of the test runs. For water, the mass balance was always within ±4%, and for 95% of the test runs, the balance was within ±3%.

Phase distribution characteristics and fluctuation characteristics at a T-junction were conducted with this apparatus. The typical results can be seen in Fig. 3, which shows some of the typical experimental results on characteristics of phase distribution and on characteristics of fluctuation in Fig. 4. The test results were described [15] in detail. So only the brief outline is given here. In the experiments concerning Fig. 4, a statistical

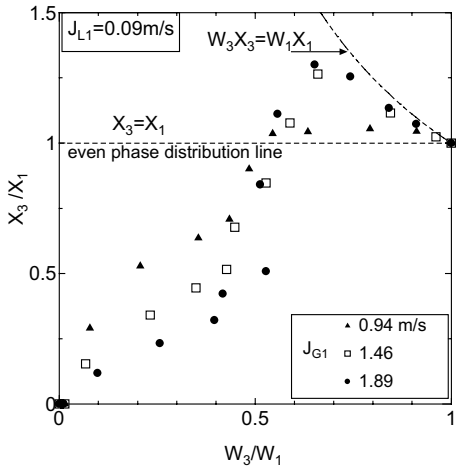

Fig. 3. Characteristic of phase distribution.

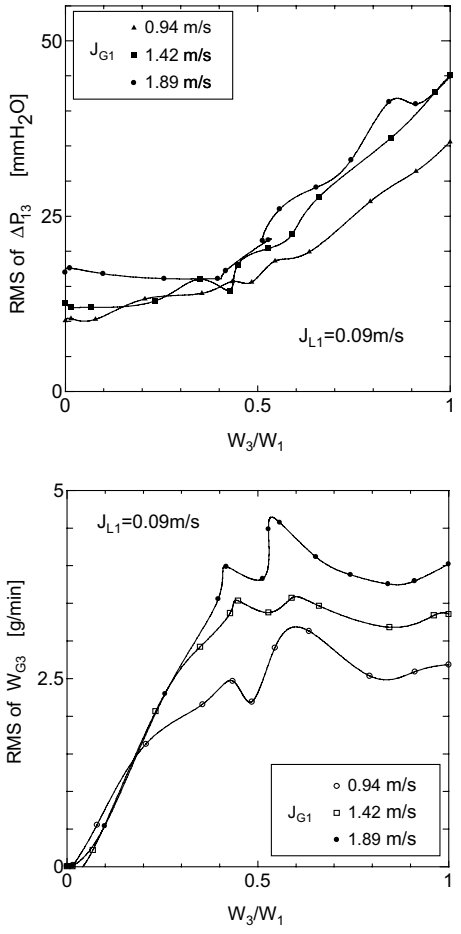

Fig. 4. RMS of ΔP_{13} and W_{G3} versus W_3/W_1.

analysis based on root mean square (RMS) was applied to temporal differential pressure signals and gas flow rate signals. The effects of the extraction flow ratio and the gas and liquid superficial velocity upstream on fluctuation characteristics of gas–liquid two-phase flow splitting at the T-junction were investigated in detail. It was found that there is a wider fluctuation in both differential pressure and gas flow rate downstream at every extraction ratio (W_3/W_1) and the fluctuation intensity increases as increasing W_3/W_1. It was also made clear that increasing either water superficial velocity or gas superficial velocity in inlet causes fluctuation more intensive while inlet flow pattern is churn flow.

This paper will focus on the nonlinear dynamic analysis of differential pressure ΔP_{13} with the extraction ratio (W_3/W_1) at 0.5 and the inlet flow pattern on bubble flow; churn flow and annular flow, respectively. Complete symmetry of the system is assumed to neglect the oscillation due to phase separation.

3. Analysis and discussions

3.1. Data range

The apparatus was operated under the following condition: inlet superficial gas velocities, J_G, ranging between 0.03 and 9.4 m/s, inlet superficial liquid velocities, J_L, ranging between 0.09 and 0.47 m/s, and mass extraction rates, W_3/W_1, from 0 to 1. All tests were carried out at nominally ambient pressure and room temperature.

All of the inlet conditions are plotted on the flow pattern map of Mishima–Ishii [16] in Fig. 5, as the inlet tube of the T-junction is vertical. As can be seen, some of the flow patterns observed in the present investigation are not consisted with the classifications calculated by the model of Mishima–Ishii [16]. The reasons are con-

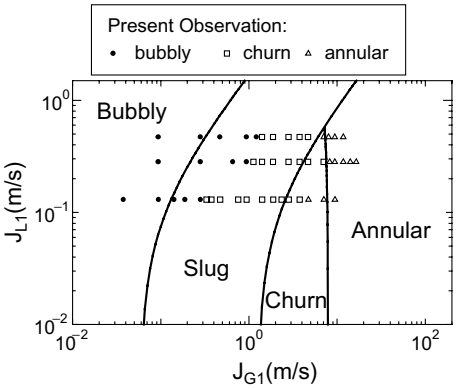

Fig. 5. Inlet conditions shown in the map of Mishima–Ishii [16].

sidered as follows: the effect of the geometry of the system, i.e. the geometric difference between a T-junction and a straight tube, the distance from observation location to the mixing room and the method for mixing two phases.

3.2. Chaotic analysis

Fig. 6 illustrates that the pressure drop fluctuations are not periodic. They are analyzed by various methods as follows.

3.2.1. Power spectral density

PSD is usually employed to extract the periodic feature of a signal. Matsui [17,18] calculated the PSD and possibility density function (PDF) of transient pressure drop signal to identify flow pattern of two-phase flow. Franca et al. [19] and Cai et al. [20] employed PSD and other fractal techniques for flow pattern identification as well. In the present work, the PSD of the differential pressure fluctuation, computed by the fast Fourier transform (FFT) technique, was used to distinguish two-phase flow through a T-junction between periodic and chaotic motion. If the power spectrum is continuous and asymptotic, the motion can be considered as chaotic [20]. Some typical results are shown in Fig. 7. It can be seen that there is no dominant frequency at all three PSD graphs. Obviously, it is asymptotic and continuous and broad-banded. So it is reasonable to consider the system as chaotic or random.

3.2.2. Pseudo-phase-plane trajectories

Another way to depict a system dynamic characteristic is to reconstruct the attractor of the selected parameter in a phase space. Not knowing the number of the freedom of the two-phase flow splitting at the T-junction, pseudo-phase-plane (embedding space) can be reconstructed with the time delay method. For the given scalar time series of the parameter, one can reconstruct D-dimensional vectors from the following equation:

$$x_i = \{x(t_i), x(t_i + \tau), x(t_i + 2\tau), \ldots, x[(t_i + (D-1)\tau]\} \tag{1}$$

where D is the embedding dimension, and τ is the time delay. The reconstructed geometrical structure has the same dimensional characteristics with the original trajectories.

Fig. 8(A–C) presents pseudo-phase-plane trajectories of the selected differential pressure for inlet bubbly flow, churn flow and annular flow. It is obvious from this three inlet flow patterns that the behavior of two-phase flow through a T-junction is chaotic. Structure of the attractor created from inlet annular flow seems to be more complex.

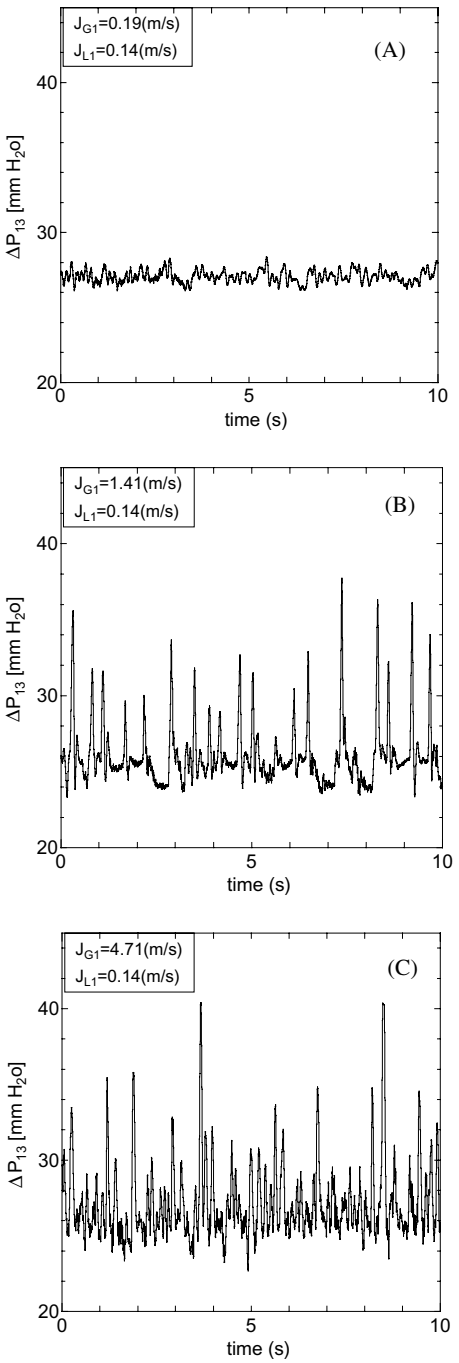

Fig. 6. Typical time series of ΔP_{13}.

3.2.3. Hurst exponent

If the degree of freedom of a system is investigated, it is usually assumed that the changes occurring in the system are of random character (Brownian motion). Examining changes of water state in the man-made lakes "Hurst" dividing the range fluctuations by standard

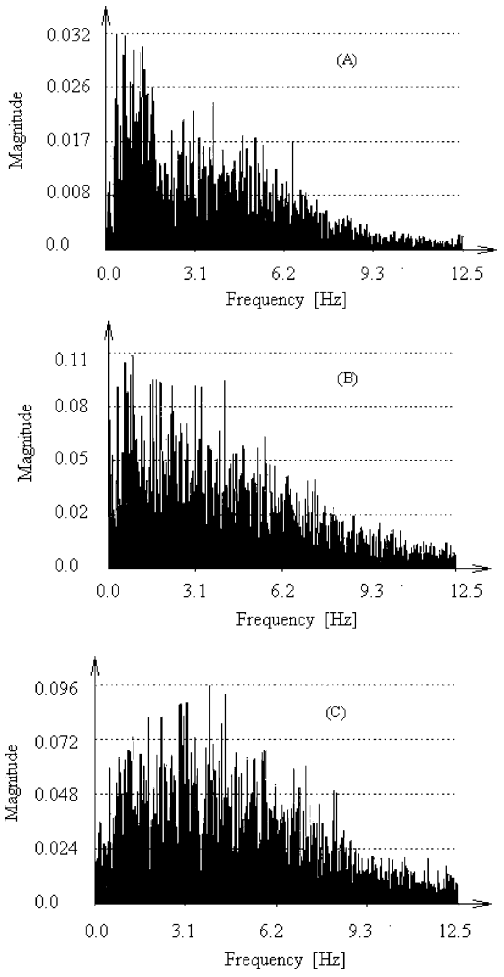

Fig. 7. Typical PSD of ΔP_{13} at various inlet flow pattern. (A) Inlet bubble flow, $J_{G1} = 0.19$ m/s, $J_{L1} = 0.14$ m/s; (B) inlet churn flow, $J_{G1} = 1.41$ m/s, $J_{L1} = 0.14$ m/s; (C) inlet annular flow, $J_{G1} = 4.71$ m/s, $J_{L1} = 0.14$ m/s.

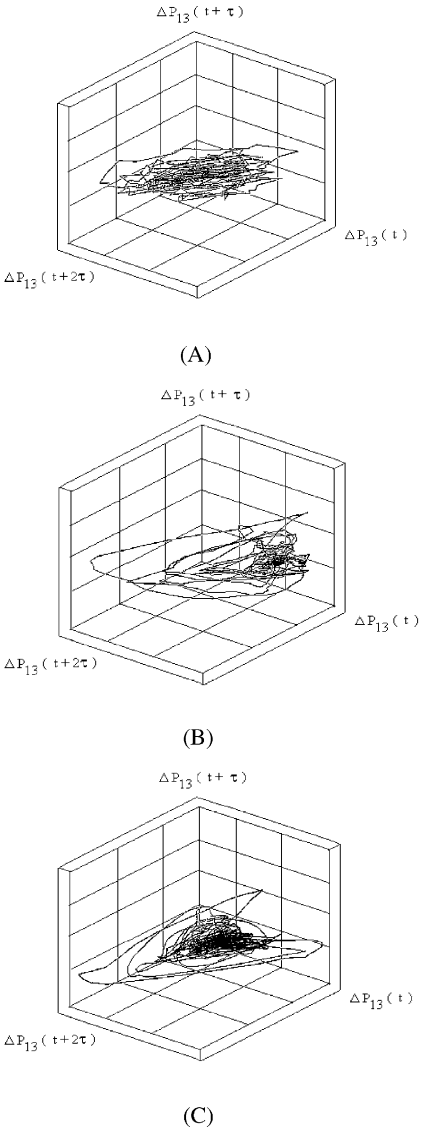

Fig. 8. Typical pseudo-phase-plane trajectories (A) for inlet bubble flow, $J_{G1} = 0.19$ m/s, $J_{L1} = 0.14$ m/s; (B) inlet churn flow, $J_{G1} = 1.41$ m/s, $J_{L1} = 0.14$ m/s; (C) inlet annular flow, $J_{G1} = 4.71$ m/s, $J_{L1} = 0.14$ m/s.

deviation of the observation, he established the non-dimensional H exponent. This kind of analysis is called the rescaled range analysis R/S [21].

Hurst exponent is determined as follows. The measured data (in the form of samples) are divided into intervals of constant number of points equal to N. For each of the intervals the following series is defined

$$T_j = \sum_{j=1}^{N} (x_j - \bar{x}_N) \tag{2}$$

For the series (2) in each interval, the R that is called range $R = \max(T_i) - \min(T_i)$ and standard deviation S are calculated. R/S characteristic for the whole time series is determined as an average of R/S calculated for all intervals of N length.

The slope of tangent to $\ln(R/S)$ in the function $\ln(N)$ gives the value of H exponent. If N number contains too many measured points, the process resembles the random motion (the long-term memory, i.e. the memory between succeeding intervals disappears). In this case the slope of the curve changes. For the signals of stochastic character $H = 0.5$ [20,21], for the chaotic system, the $H > 0.5$. Border point N^* between the area where the $H > 0.5$ and the area where $H = 0.5$ corresponds with the boundary of the natural period of a physical system.

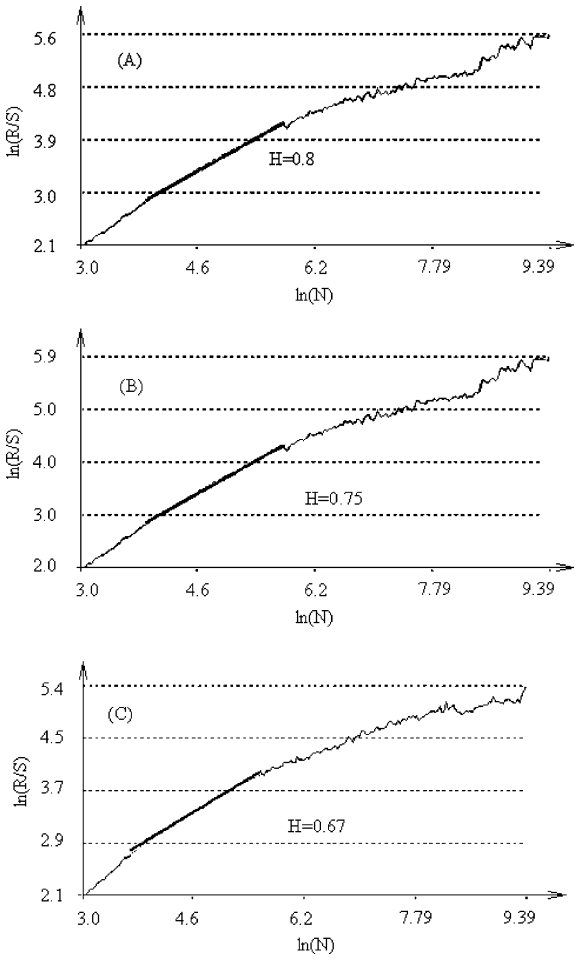

Fig. 9. Typical Hurst exponents (H) of various inlet flow patterns. (A) Inlet bubble flow, $J_{G1} = 0.19$ m/s, $J_{L1} = 0.14$ m/s; (B) inlet churn flow, $J_{G1} = 0.19$ m/s, $J_{L1} = 1.41$ m/s; (C) inlet annular flow, $J_{G1} = 4.71$ m/s, $J_{L1} = 0.14$ m/s.

Fig. 9 shows the rescaled range $\ln(R/S)$ plotted against $\ln(N)$ for different flow patterns. The slope of the straight lines, drawn arbitrarily close to the saturation value for the rescaled range curve, indicates the deterministic nature of the flow. The values of the Hurst exponent H ranged from 0.72 to 0.87 for inlet bubble flow, from 0.7 to 0.97 for inlet churn flow, approximately constant 0.67 for inlet annular. Fig. 10 shows Hurst exponent (H) versus gas superficial velocity at each test run. As can be seen, all of the Hurst dimensions are larger than 0.5. It suggests that the behavior of the system has deterministic chaos character. The value of Hurst exponent (H) indicates that the behavior of system is different from stochastic behavior. Obtained results show that differential pressure fluctuations in case of annular flow are closer to stochastic behavior than other kinds of flows.

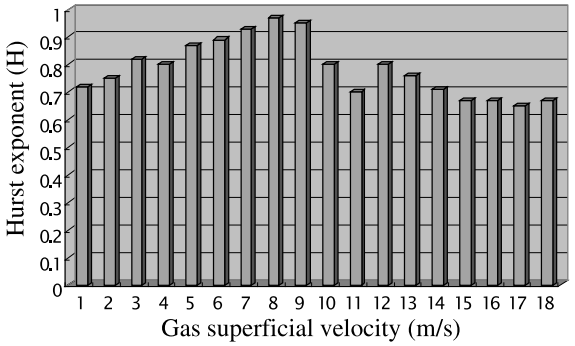

Fig. 10. Gas superficial velocity versus Hurst exponent (H) at each test run.

3.2.4. Largest Lyapunov exponents

Lyapunov exponents, the average exponential rates of divergence or convergence of nearby orbits in phase space, have been shown to be the most useful dynamic diagnostic tool in quantifying chaotic systems [20].

For the measured data in the form of time series:

$$\{x_n\} = \{x_1, x_2, \ldots, x_n\} \tag{3}$$

determination of all Lyapunov exponents is not possible. It is, however, possible to determine the value of the largest Lyapunov exponent. In this case, on the attractor immersed in D dimensional space, two closest points situating at a distance of at least one orbiting period one from another, are selected. The distance between the points is represented by $L(t_j)$. Thus, the distance of the selected points after the passage of some evolution time is calculated, and the new distance of the pair of points is $L(t_{j+1})$. The largest Lyapunov exponent is calculated according to the formula [21]:

$$\lambda_1 = \frac{1}{t}\sum_{j=1}^{m} \log_2 \frac{L(t_{j+1})}{L(t_j)} \tag{4}$$

where m is the number of point pairs examined, t the time of evolution.

The largest Lyapunov exponent can be determined when such characteristics of attractor as fractal dimension, average orbiting time and time-delay are known. For a long time series, the results of calculation of λ_1 approach stable value, being an estimation of the largest value of Lyapunov exponent. The calculation of the largest Lyapunov exponent is possible only if the fractal dimension of the attractor is known.

While $\lambda_l > 0$, the motion is chaotic; while $\lambda_l = 0$, the motion is regular. The value of λ_l is a criterion for chaos. Fig. 11(A–C) shows largest Lyapunov exponents for bubble flow; churn flow and annular flow. The exponents are positive, which provides further evidence of chaotic behavior of two-phase flow through a T-junction.

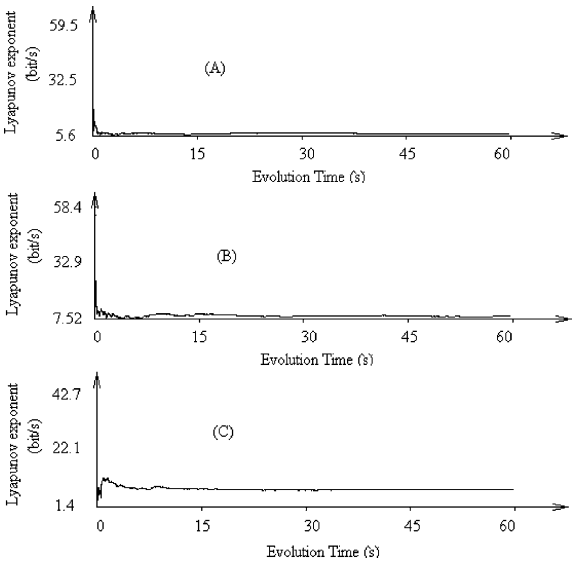

Fig. 11. Typical largest Lyapunov exponents of various inlet flow patterns. (A) Inlet bubble flow, $J_{G1} = 0.19$ m/s, $J_{L1} = 0.14$ m/s; $\lambda = 6.55$, (B) inlet churn flow, $J_{G1} = 1.41$ m/s, $J_{L1} = 0.14$ m/s; $\lambda = 8.69$, (C) inlet annular flow, $J_{G1} = 4.71$ m/s, $J_{L1} = 0.14$ m/s; $\lambda = 7.78$.

The value of largest Lyapunov exponent describes the rate of information loss about the system. The calculated value of $1/\lambda_l[\text{bit/bit/s}] \approx 1/6.55 = 0.15$ [s] (in case of bubble flow) shows how long a initial condition influences the flow. The value of the largest Lyapunov exponent is also a measure of chaos level in the system. Results of calculations indicate that the rate of information loss is bigger in the churn flow. In other words, we can say that the value of the largest Lyapunov exponent is a measure of correlations between the two-phase flow in the vertical inlet pipe and horizontal branch pipe. Results of calculation indicate that when the flow pattern upstream changes to churn flow, the two-phase flow in vertical and horizontal pipe becomes independent. It is consistent with the observation very well since the flow pattern in horizontal tube is stratified-wavy flow.

3.2.5. Correlation dimensions

The trajectories of the chaotic system in the phase space do not form any single geometrical object such as circle or torus, but form objects called strange attractors of the structure resembling the one of a fractal. One of the essential characteristics of fractals is their dimension [21,23–25]. For experimental data, the correlation dimension D is defined by the following expression [22]:

$$D = \lim_{l \to 0} \frac{1}{\ln l} \ln C(l) \tag{5}$$

$$C(l) = \lim_{N \to \infty} \frac{1}{N^2} \sum_{i,j} \Theta(l - |x_i - x_j|) \tag{6}$$

where Θ is the Heaviside's step function determines the number of attractor's point pairs of the distance shorter than l. Fractal dimension is calculated by determining the value of the slope of the regression line crossing a middle region of the curve C [23]. For the stochastic signal the fractal dimension increases with the increase of the embedding dimension. If the signal examined is of deterministic chaos character, then the value of a slope of the regression line approaches constant value D. The

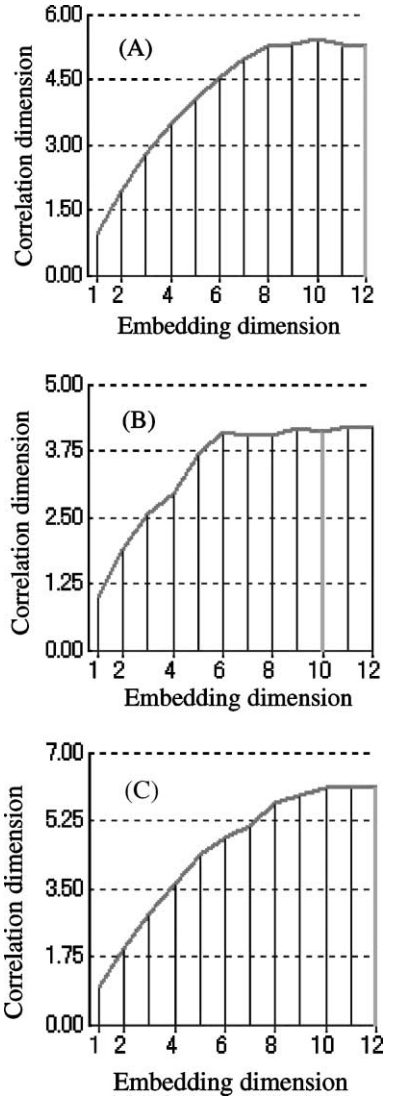

Fig. 12. Typical correlation dimension of various inlet flow patterns. (A) Inlet bubble flow, $J_{G1} = 0.19$ m/s, $J_{L1} = 0.14$ m/s; (B) inlet churn flow, $J_{G1} = 1.41$ m/s, $J_{L1} = 1.41$ m/s; (C) inlet annular flow, $J_{G1} = 4.71$ m/s, $J_{L1} = 0.14$ m/s.

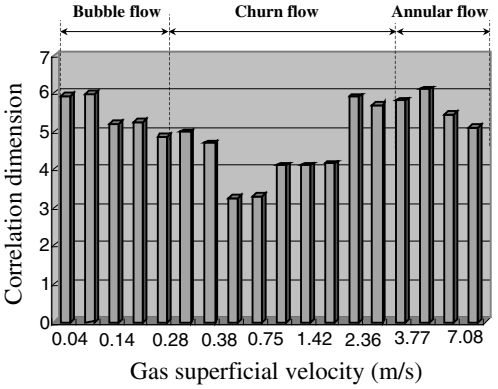

Fig. 13. Gas superficial velocity versus correlation dimension at each test run (liquid superficial velocity $J_{L1} = 0.14$ m/s).

value determines the correlation dimension of the attractor investigated. Calculation of the correlation dimension is being done for the embedding dimension $M > 2D + 1$, where D is the correlation dimension of the attractor considered [24].

Fractal dimension, including the capacity dimension, correlation dimension, and information dimension, provides a measure of the minimum degree of freedom and thus provides a quantitative measure of the complexity of the phenomena [26,27]. The estimated correlation dimensions versus the embedding dimensions for inlet bubble flow; churn flow, and annular flow are shown in Fig. 12. It indicates that the system is more complex than at inlet bubble flow and annular flow than at inlet churn flow. Fig. 13 shows correlation dimensions versus gas superficial velocity of all tests run with liquid superficial velocity $J_{L1} = 0.14$ m/s. It exhibits that two-phase flow splitting at a T-junction is not a random oscillation but a deterministic chaotic motion.

4. Summary

Several measurement methods that are used in chaos theory were employed to analyze differential pressure fluctuation of two-phase flow through a T-junction. These methods included: PSD function, Hurst exponent, the largest Lyapunov exponents, correlation dimensions and pseudo-phase-plane trajectories. Three kinds of inlet flow patterns including bubble flow, churn flow and annular flow, were investigated. It is demonstrated that two-phase flow splitting at a T-junction is a complicated nonlinear dynamic system by the analysis on time series of differential pressure. Namely, PSD is asymptotic and continuous and band-broad indicates the existence of chaotic behavior. The Hurst exponent is larger than 0.5 showing that the flow behaviors studied are chaotic but random. The value of the lagerst Lyapunov exponent allows identifying the loss of correlation between the dynamics of two-phase flow in the vertical and horizontal pipes. Correlation dimensions quantify the identified chaotic behavior. Thus, this study provided new viewpoints to well understand the behaviors of two-phase flow through a T-junction. It will also be significant for establishing valid models in the future that are different from conventional ones.

References

[1] B.J. Azzopardi, Two-phase flow in junctions. Encyclopedia of Fluid Mechanics, vol. 3, Gulf Publishing, New York, 1986 (Chapter 25).
[2] R.T. Lahey, Current understanding of phase separation mechanisms in branch conduits, Nucl. Eng. Des. 95 (1986) 145–161.
[3] U. Muller, J. Reimann, Redistribution of two-phase flow in branching conduits: a survey. Presented at the Int. Conf. Multiphase flows, Tsukuba, Japan, 1991.
[4] B.J. Azzopardi, E. Hervieu, Phase separation at T-junctions, Presented at the 3rd Int. Workshop on Two-phase Flow, London, UK, 1992.
[5] B.J. Azzopardi, Phase separation at T-junctions, Multiphase Sci. Technol. 11 (1999) 223–329.
[6] N. Saba, R.T. Lahey, The analysis of phase separation phenomena in branching conduits, Int. J. Multiphase Flow 10 (1984) 1–20.
[7] J. Reimann, W. Seeger, Two-phase flow in a T-junction with a horizontal inlet—Part II: Pressure differences, Int. J. Multiphase Flow 12 (1986) 587–608.
[8] S.T. Hwang, R.T. Lahey, Phase separation in dividing two-phase flows, Int. J. Multiphase Flow 14 (1988) 439–458.
[9] J.D. Ballyk, M. Shoukri, A.M.C. Chan, Steam-water annular flow in a horizontal dividing T-junction, Int. J. Multiphase Flow 20 (1994) 819–836.
[10] J.R. Ruell, H.M. Soliman, G.E. Sims, Two-phase flow pressure drop and phase distribution at a horizontal tee junction, Int. J. Multiphase Flow 20 (1994) 819–836.
[11] L.C. Walters, H.M. Soliman, G.E. Sims, Two-phase pressure drop and phase distribution at reduced tee junctions, Int. J. Multiphase Flow 24 (1998) 755–792.
[12] A.E. Fouda, E. Rhodes, To-phase annular flow stream division in a simple tee, Trans. Inst. Chem. Eng. 52 (1974) 354–360.
[13] L.H. Chai, X.F. Peng, B.X. Wang, Nonlinear aspects of boiling systems and a new method for predicting the pool nucleate boiling heat transfer, Int. J. Heat Mass Transfer 43 (2000) 75–84.
[14] L.H. Chai, M. Shoji, Boiling curves-bifurcation and catastrophe, Int. J. Heat Mass Transfer 44 (2001) 4175–4179.
[15] S.F. Wang, M. Shoji, Fluctuation characteristics of two-phase flow splitting at a vertical impacting T-junction, Int. J. Multiphase Flow, in press.
[16] M. Mishima, M. Ishii, Flow regime transition criteria for upward two-phase flow in vertical tubes, Int. J. Heat Mass Transfer 27 (1984) 723–737.
[17] G. Matsui, Identification of flow regimes in vertical gas liquid two-phase flow using differential pressure fluctuations, Int. J. Multiphase Flow 10 (1984) 711–720.

[18] G. Mastui, Automatic identification of flow regimes in vertical two-phase flow using differential pressure fluctuations, Nucl. Eng. Des. 95 (1986) 221–231.
[19] F. Franca, M. Acikgoz, R.T. Lahey Jr., A. Clausse, The use of fractal techniques for flow regime identification, Int. J. Multiphase Flow 17 (1991) 545–552.
[20] Y. Cai, M.W. Wambsganss, J.A. Jendrzejczyk, Application of chaos theory in identification of two-phase flow patterns and transitions in a small, horizontal, rectangular channel, ASME J. Fluid Eng. 118 (1996) 383–390.
[21] E.E. Peters, Chaos and Order in the Capital Markets. A New View of Cycle, Prices, and Market Volatility. Wiley, New York, 1996.
[22] T. Martyn, Fractals and its visualisation algorithms, Nakom, Poznan, 1996 (in Polish).
[23] H.G. Schuster, Deterministic Chaos, An Introduction, VCH, Weinheim, 1989.
[24] T.S. Parker, L.O. Chua, Chaos: A tutorial for engineers. Proceedings of the IEEE, 75 (8) (1987) 982–1008.
[25] J. Kudrewicz, Fractal and Chaos, WNT, Warszawa, 1993 (in Polish).
[26] M. Shoji, Boiling chaos and modeling, Heat Transfer 1998, Proceedings of the 11th IHTC, vol. 1, Talor & Francis, London, 1998, pp. 3–21.
[27] L.H. Chai, M. Shoji, Dry patch interaction caused by lateral conduction in transition boiling, Int. J. Heat Mass Transfer 44 (2001) 4169–4173.